Applications of higher-order phase shifting algorithms for multiple-wavelength metrology

Upputuri, Paul Kumar; Pramanik, Manojit

2019

Upputuri, P. K., & Pramanik, M. (2019). Applications of higher-order phase shifting algorithms for multiple-wavelength metrology. Proceedings of SPIE - Quantitative Phase Imaging. doi:10.1117/12.2511942

https://hdl.handle.net/10356/104906

https://doi.org/10.1117/12.2511942

Applications of higher-order phase shifting algorithms for multiple-wavelength metrology

Paul Kumar Upputuri*, and Manojit Pramanik
School of Chemical and Biomedical Engineering, Nanyang Technological University, Singapore 637459

ABSTRACT

Multiple-wavelength interferometric techniques have been successfully used for large step-height and large deformation measurements. Also it could resolve the step height between smooth and rough surfaces which is not possible with single wavelength interferometry. Temporal phase shifting algorithm, which requires a phase shifter such as PZT, has been widely used for accurate phase evolution in interferometry. The phase shifter needs to be calibrated at every wavelength if multiple wavelengths are used for measurement, it is a time consuming process. If phase shifter is not calibrated accurately, it can introduce phase shift errors. In this work, we will discuss various phase shifting algorithms, and their tolerance for phase shift error. And the applications of higher-order phased shifting algorithms will be presented. The study is useful for multiple-wavelength and white light interferometry where more than one wavelength is used for optical phase measurements.

***Keyword*:** Phase shifting interferometry, multiple-wavelength, surface profiling, step-height, deformation

1. INTRUDUCTION

Interferometry is a non-contact high-sensitive optical tool for optical metrology. It is widely used in all kinds of scientific and engineering applications for making accurate measurements. It can measure surface roughness, surface deformation, step height or depth on the surface, surface/sub-surface defects, refractive index, vibration modes of mechanical structures, etc. [1-6] Interferometry can inspect smooth (reflective) and rough (speckled) objects under static, quasi-static or dynamic conditions [7-11]. In case of smooth surfaces, interference fringes are directly generated if there is an optical path difference between the object and reference arms. But in case of rough surfaces, to generate fringes the speckle pattern before and after deformation needs to be subtracted. The interferometry that can handle rough surfaces is known as speckle interferometry or TV holography [12]. So in interferometry, the information about the surface is encoded in the fringe pattern, which represents the phase distribution. By analysing the fringe pattern, qualitative information can be obtained. For quantitative information and sign of the surface or deformation, the phase information needs to be calculated from the fringes.

Quantitative fringe analysis methods include single frame methods such as Fourier transform [13], Hilbert transform, etc. [9, 14-17] and multiple frame methods such as temporal phase shifting, polarization phase shifting etc. [18, 19] A phase shifting technique converts the fringe pattern into a phase distribution image and it can resolve displacement below lambda/100. Temporal phase shifting technique (PST) is widely used for static fringe analysis. This approach was successfully implemented in single wavelength [4], two-wavelength [20-23], three-wavelength [24, 25], white light interferometry [17, 26-30], etc. Single wavelength measurements are accurate, but using one wavelength greatly limits the wide spread applications of interferometry. The major drawback associated with such techniques is that the unambiguous step-height measurement range is limited to half-a-wavelength ($\lambda/2$) and also shape of rough surface cannot be obtained. So later to overcome these problems, two or more wavelengths were used in advanced interferometers. These multiple wavelength methods can extend the unambiguous range of interferometer for step-height measurement, can reveal the shape of speckled surface, and also allows large deformation measurements. To implement PST, a calibrated PZT is used to introduce known phase shift between object and reference beams. The phase shift is wavelength dependent, *i.e.*, if wavelength is changed the PZT need to be recalibrated. If single wavelength is used for measurements, PZT can be precisely calibrated for phase shift and use simple monochrome CCD to acquire fringe pattern. But if two or three laser wavelengths are used for phase measurement, the PZT needs to be calibrated at each

* Email: upputuri@ntu.edu.sg

wavelengths which otherwise introduces a phase shift error at other wavelengths. If white light is used it is even difficult to calibrate the PZT at all the wavelengths. The use of colour CCD makes it possible to implement temporal PST in white light interferometry [30, 31]. To compensate for the phase shift errors, several phase shifting algorithms were developed. In this we will discuss the widely used phase shifting algorithms, their tolerance for phase shift errors and their applications in multiple-laser interferometry and white light interferometry.

2. TEMPORAL PHASE SHIFTING ALGORITHMS

Interferometer generates fringe pattern related to the surface of the test object. The fringe equation contains three unknowns: the amplitude of the reference beam, the amplitude of the object beam, and the phase difference between object and reference beams. So, three equations are required to solve the interference equation for phase difference, it is related to the parameters of interest, *i.e.*, surface height, deformation etc. The interference between the smooth reference and object beams results in a visible fringe pattern which can be written as

$$I = I \tag{1}$$

where I_o is the bias intensity, V is the fringe contrast, $\phi = (4\pi/\lambda)z$ is the phase at the wavelength λ, z is the profile height or depth. The intensity distribution of fringes obtained at multiple wavelengths can be written as

(2)

where $\phi_i = (4\pi/\lambda_i)z$ is the phase at λ_i. Implementing phase shifting technique requires three or more frames for desired phase calculation. The intensity distribution of phase shifted frames at multiple-wavelengths can be written as [32, 33]

(3)

where N is the number of the phase shifted frames, and α_i is the phase shift at λ_i. Depending on the algorithm type, the phase shifted frame are store. For example, to implement 8-step algorithm, eight phase shifted frames at 0, π/2, π, 3π/2, 2π, 5π/2, 3π, 7π/2 phase shift. The phase shifting formulas 3-step to 8-step for π/2 phase shift are discussed in detail in Ref. [31, 34-38]. The type of algorithm and their tolerance for phase shift error are listed in Table-1. The algorithms 3, 4a provide zero tolerance, on the other hand 8-step algorithm shows maximum ±20% tolerance [21, 24, 25].

S.No.	Type of phase Stepping algorithm	Tolerance (%)
1	3-step	0
2	4a-step	0
3	4b-step	±3
4	5-step	±3
5	6-step	±10
6	7-step	±10
7	8-step	±20

Table 1. Types of phase shifting algorithms, phase evaluation equations, and their percentage tolerance for phase shift error. The phase shift chosen here is π/2.

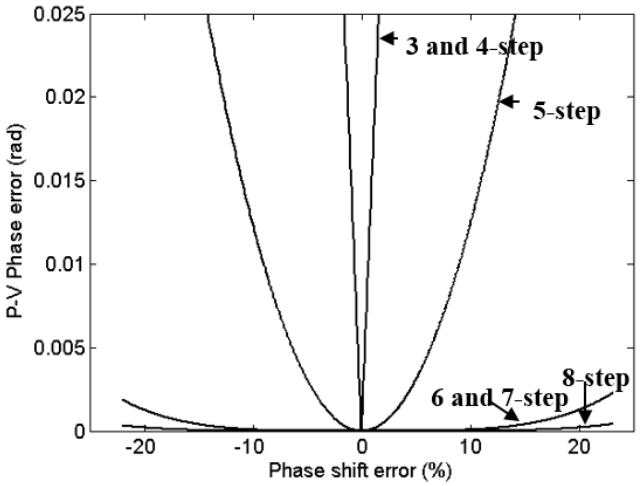

Fig. 1. Peak-to-valley (P-V) phase error in the calculation of phase due to phase shift error in different algorithms. Tolerance for phase shift error is maximum for 8-step method.

4. MULTIPLE-WAVELENGTH INTEROMETRY

In multiple-wavelength techniques, more than one wavelength is used for surface profiling. Temporal PST was implemented in white light interferometry [Fig. 2(a)] with RGB CCD camera for surface profiling of large discontinuities [30]. A typical white light fringe pattern on a tilted smooth surface acquired with a single chip RGB CCD camera is shown in Fig. 2(a). Each wavelength in white light, will generate its own pattern, hence the resultant of the entire fringe pattern looks like an envelope. The system includes a halogen lamp and a 1-chip RGB CCD that has three spectral bands around red (620 nm), green (540 nm), blue (460 nm). The halogen lamp can generate broad band, but the wavelengths are selected by the CCD. To implement phase shifting technique, the PZT attached to the Mirau objective was calibrated for $\pi/2$ phase shift at 560 nm. If a phase shifter (such as PZT) is calibrated for a known phase shift of 90 at wavelength λ_{cal}, and same motion of the PZT is used for other wavelengths (λ_i), then the phase error introduce at all other λ_i wavelengths can be expressed as $\alpha_i = (\lambda_{cal}/\lambda_i)90^o$. The PZT is calibrated at $\lambda 2 = 560$ nm for phase shift $\alpha 2 = 90^o$. Then, the phase shift values become $\alpha 1 = (\lambda 2/\lambda 1)\ 90^o = 78.4^o$ for $\lambda 1 = 620$ nm and $\alpha 3 = (\lambda 2/\lambda 3)\ \pi/2 = 105.7^o$ for $\lambda 3 = 450$ nm. Here the maximum error involved is ~16^o which can be compensated by using eight step algorithm (Table-1).

Similarly, eight algorithm can be used for phase calculation in multiple-wavelength laser interferometer [Fig. 2(b)]. It can provide shape as well as large deformation measurements. The system includes three lasers (He-Ne laser@632.8 nm, Nd:YAG laser@532 nm, He-Cd laser@441.6 nm). A typical fringe pattern obtained by simultaneously illuminating all three R, G, B coloured wavelengths on a tilted smooth surface is shown in Fig. 2(b). To implement temporal PST here, the phase shifter is calibrated for phase shift $\pi/2$ at 532 nm. Then, the phase shift values at 632.8 nm, 441.6 nm become 75.7^o, 108.4^o respectively. So here the maximum error involved is ~18^o which can be compensated by 8-step algorithm. Thus the phase shift algorithm can be chosen based on the amount of phase shift error expected during phase shifting from the nominal value of $\pi/2$. Phase shift errors as large as 20^o can be compensated using 8-step algorithm.

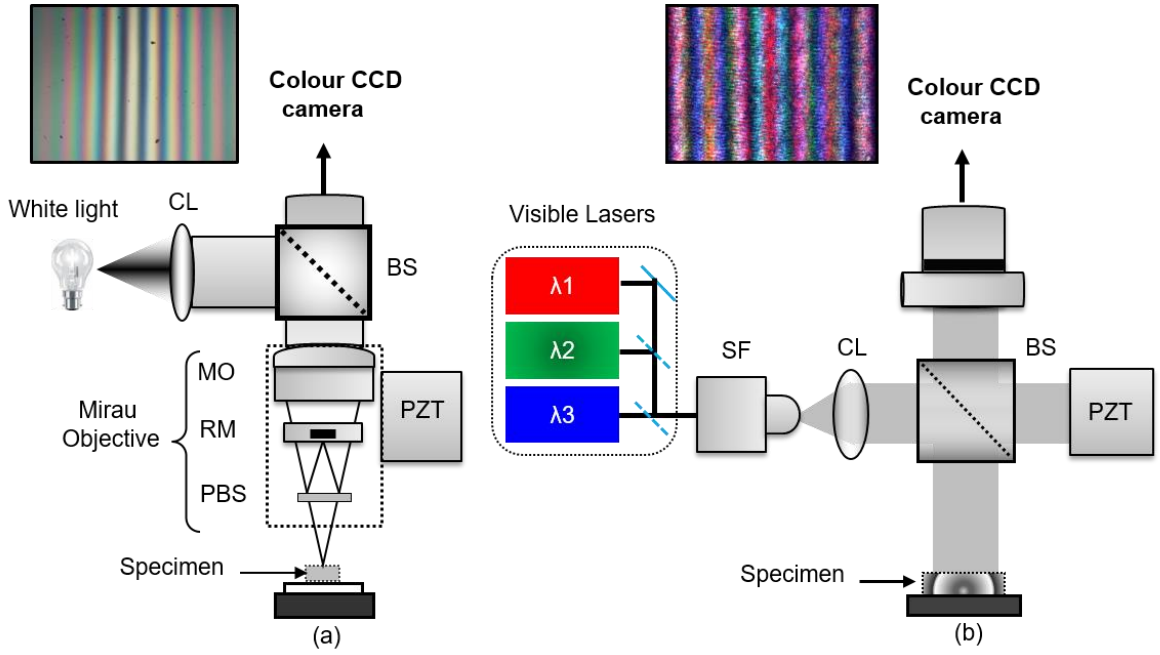

Fig. 2. Schematic drawing of colour CCD camera based (a) Mirau white light interferometer, and (b) multiple-wavelength laser interferometer. Here SF- Spatial filter setup, CL- collimating lens, BS- Beam splitter, PZT- Piezoelectric transducer, MO- Microscopic objective, RM- Reference mirror, PBS- Partially reflecting beam splitter. Here, $\lambda 1 = 632.8$ nm (Red laser), $\lambda 2 = 532$ nm (Green laser), $\lambda 3 = 441.6$ nm (Blue laser).

4. MEASUREMENT OF TILT ON SPECKLE SURFACE

The system in Fig. 2(b) was demonstrated for the tilt measurement on a rough surface. A flat rough sample was placed in the system and was illuminated by the three lasers simultaneously. Speckle patterns before and after tilting the sample

were acquired using colour CCD camera. The use of colour CCD allows simultaneous illumination and it makes the data acquisition simple. After separating the speckle patterns at individual wavelengths, the corresponding wrapped phase maps were calculated using 8-step algorithm to compensate for the phase shift error involved. The phase maps at individual wavelength are shown in Figs. 3(a-c). If tilt is small, *i.e.*, less number of fringes then single wavelength phase provides accurate phase profile. If the tilt is large, *i.e.*, more number of fringes at single wavelength sometimes may result in ambiguity. In such cases, the individual phase maps are subtracted to generate phase maps at effective wavelengths as shown in Figs. 3(d,e). In phase subtraction method, the phase at one wavelength is subtracted from that of the other to generate phase at an effective wavelength $\Lambda_{12}(=\lambda_1\lambda_2/|\lambda_1-\lambda_2|)$ [22, 39]. The effective phase is then unwrapped to get the continuous phase map which is shown in 3D mesh plot [Fig. 3(f)]. The line profile across the sample is shown in Fig. 3(g) which has maximum tilt ~11.8 µm. In out-of-plane configuration this tilt corresponds to ~44 fringes at 532 nm.

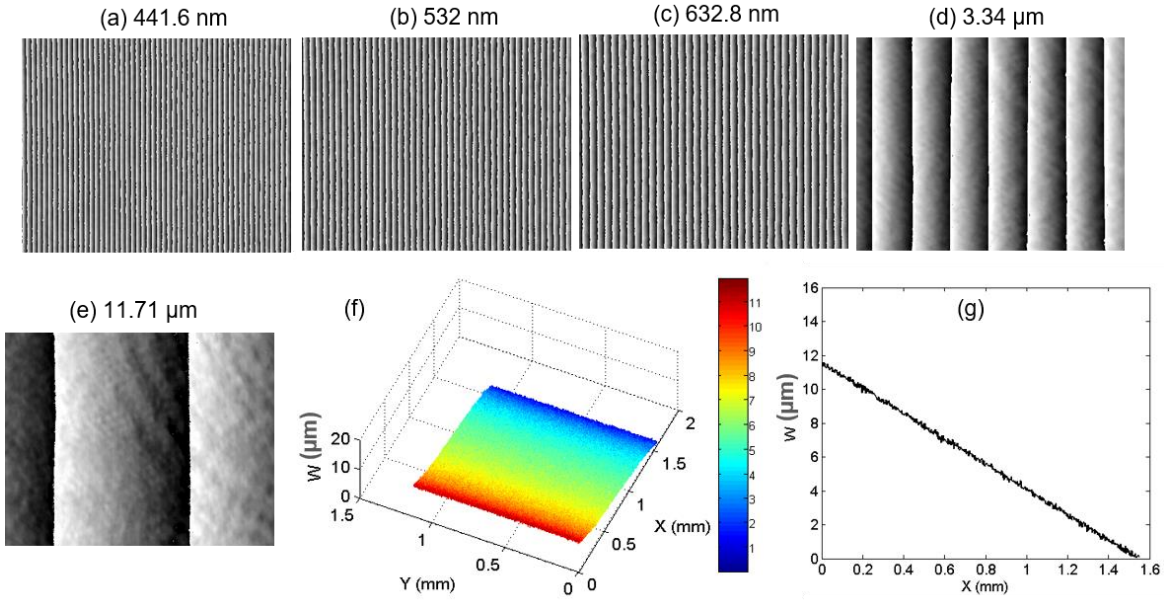

Fig. 3. Measurement of large-tilt on rough sample using multiple-wavelength laser interferometry: wrapped phase maps corresponding to interferograms at (a) 441.6 nm, (b) 532 nm, (c) 632.8 nm, wrapped phase maps at effective wavelength (d) 3.34 µm, (e) 11.71 µm, (f) 3D tilt profile, (g) line scan profile showing large tilt ~11.8 µm, which corresponds to approximately 44 fringes at 532 nm.

5. CONCLUSIONS

In this article, we discussed various phase shifting algorithms, and their tolerance for phase shift error. The lower-order algorithms such as 3 and 4a step methods provide zero tolerance for phase shift error, whereas 4b, 5 methods show ±3%, 6, 7 methods show ±10%, and 8-step method provides ±20%. Here 3-step and 4a-step, require less number of frames for phase calculation but the PZT need to be calibrated accurately which otherwise introduces error in the final phase. Calibrating PZT accurately may be time consuming process. If PZT is calibrated for single wavelength, phase shift error involved is less, and then 5-step method would be sufficient. Phase shift errors as large as 20^o can be compensated using 8-step algorithm. For RGB interferometry where large errors are expected, 8-step would be useful. Thus the phase shift algorithm can be chosen based on the amount of phase shift error expected during phase shifting from the nominal value of $\pi/2$. Tilt measurement on rough surface with multiple-wavelength (RGB) laser interferometer was demonstrated using 8-step method.

ACKNOWLEDGMENT

The authors would like to acknowledge the financial support from the Singapore Ministry of Health's National Medical Research Council (NMRC/OFIRG/0005/2016: M4062012).

REFERENCES

[1] D. Malacara, [Optical Shop Testing] John Wiley & Sons, Inc., 674-763 (2007).

[2] U. Paul Kumar, N. Krishna Mohan, and M. P. Kothiyal, "Measurement of static and vibrating microsystems using microscopicTV holography," Optik - International Journal for Light and Electron Optics, 122(1), 49-54 (2011).

[3] W. Osten, [Optical inspection of Microsystems] CRC Press, Boca Raton, FL(2006).

[4] U. Paul Kumar, B. Bhaduri, N. Krishna Mohan *et al.*, "Microscopic TV holography for MEMS deflection and 3-D surface profile characterization," Optics and Lasers in Engineering, 46(9), 687-694 (2008).

[5] U. P. Kumar, M. P. Kothiyal, and N. K. Mohan, "Microscopic TV shearography for characterization of microsystems," Optics letters, 34, 1612-1614 (2009).

[6] U. P. Kumar, N. K. Mohan, and M. P. Kothiyal, "Microscopic TV sherography for microsystems characterization," Proceedings of SPIE, 7432, 74320T-74320T-8 (2009).

[7] P. K. Upputuri, and M. Pramanik, "Microsphere-aided optical microscopy and its applications for super-resolution imaging," Optics Communications, 404, 32-41 (2017).

[8] B. Bhaduri, N. K. Mohan, and M. P. Kothiyal, "A dual-function ESPI system for the measurement of out-of-plane displacement and slope," Optics and Lasers in Engineering, 44(6), 637-644 (2006).

[9] U. Paul Kumar, U. Somasundaram, M. P. Kothiyal *et al.*, "Single frame digital fringe projection profilometry for 3-D surface shape measurement," Optik - International Journal for Light and Electron Optics, 124(2), 166-169 (2013).

[10] U. P. Kumar, N. K. Mohan, and M. P. Kothiyal, "Time average vibration fringe analysis using Hilbert transformation," Applied Optics, 49, 5777-5786 (2010).

[11] U. P. Kumar, Y. Kalyani, N. K. Mohan *et al.*, "Time-average TV holography for vibration fringe analysis," Applied Optics, 48, 3094-3101 (2009).

[12] A. F. Doval, "A systematic approach to TV holography," Measurement Science and Technology 11, R1-R36 (2000).

[13] B. Bhaduri, M. P. Kothiyal, and N. Krishna Mohan, "Curvature measurement using three-aperture digital shearography and fast Fourier transform," Optics and Lasers in Engineering, 45(10), 1001-1004 (2007).

[14] U. P. Kumar, N. K. Mohan, and M. P. Kothiyal, "Characterization of micro-lenses based on single interferogram analysis using Hilbert transformation," Optics Communications, 284(21), 5084-5092 (2011).

[15] G. Goldstein, and K. Creath, "Dynamic 4-dimensional microscope system with automated background leveling," Proc SPIE Int Soc Opt Eng, 8493, 84930N (2012).

[16] K. Kitagawa, "Single-shot surface profiling by multiwavelength interferometry without carrier fringe introduction," Journal of Electronic Imaging, 21(2), 021107 (2012).

[17] P. K. Upputuri, M. Pramanik, K. M. Nandigana *et al.*, "White light single-shot interferometry with colour CCD camera for optical inspection of microsystems," Proceedings of SPIE, 9524, 95240C-1-95240C-8 (2015).

[18] S. Rothau, C. Kellermann, S. Mayer *et al.*, "Polarization and phase-shifting interferometry for arbitrary, locally varying polarization states," Applied Optics, 56(5), (2017).

[19] M. Servin, J. C. Estrada, and J. A. Quiroga, "The general theory of phase shifting algorithms," Optics Express 17(24), 21867-21881 (2009).

[20] C. Polhemus, "Two-Wavelength Interferometry," Applied Optics, 12, 2071-2074 (1973).

[21] P. K. Upputuri, S. Umapathy, M. Pramanik *et al.*, "Use of two wavelengths in microscopic TV holography for non destructive testing," Optical Engineering, 53, 110501-1-110501-3 (2014).

[22] U. P. Kumar, B. Bhaduri, M. P. Kothiyal *et al.*, "Two-wavelength micro-interferometry for 3-D surface profiling," Optics and Lasers in Engineering, 47(2), 223-229 (2009).

[23] P. K. Upputuri, M. Pramanik, M. P. Kothiyal *et al.*, "Two-wavelength microscopic speckle interferometry using colour CCD camera," Proceedings of SPIE, 9302, 93023K-1-93023K-6 (2015).

[24] U. P. Kumar, N. K. Mohan, and M. P. Kothiyal, "Deformation and shape measurement using multiple wavelength microscopic TV holography," Optical Engineering, 48(2), 023601-1-023601-10 (2009).

[25] P. K. Upputuri, N. K. Mohan, and M. P. Kothiyal, "Measurement of discontinuous surfaces using multiple-wavelength interferometry," Optical Engineering, 48(7), 073603-1-073603-8 (2009).

[26] Z. Lei, X. Liu, L. Chen *et al.*, "A novel surface recovery algorithm in white light interferometry," Measurement, 80, 1-11 (2016).

[27] F. Fang, Z. Zeng, X. Zhang *et al.*, "Measurement of micro-V-groove dihedral using white light interferometry," Optics Communications, 359, 297-303 (2016).

[28] P. K. Upputuri, M. Pramanik, K. M. Nandigana *et al.*, "White light interferometer with color CCD for 3D-surface profiling of microsystems," Proceedings of SPIE, 9302, 93023R-1-93023R-6 (2015).
[29] P. K. Upputuri, L. Gong, H. Wang *et al.*, "Measurement of large discontinuities using single white light interferogram," Opt Express, 22(22), 27373-80 (2014).
[30] U. P. Kumar, W. Haifeng, N. K. Mohan *et al.*, "White light interferometry for surface profiling with a colour CCD," Optics and Lasers in Engineering, 50(8), 1084-1088 (2012).
[31] P. K. Upputuri, M. Pramanik, K. M. Nandigana *et al.*, "Multi-colour microscopic interferometry for optical metrology and imaging applications," Optics and Lasers in Engineering, 84, 10-25 (2016).
[32] U. P. Kumar, N. K. Mohan, M. P. Kothiyal *et al.*, "Deformation analysis on micro objects using multiple wavelength microscopic TV holography," Proceedings of SPIE, 7155, 71550D-71550D-12 (2008).
[33] U. Paul Kumar, N. Krishna Mohan, and M. P. Kothiyal, "Multiple wavelength interferometry for surface profiling," Proceedings of SPIE, 7063, 70630W-1-70630W-10 (2008).
[34] K. Creath, "Phase-shifting speckle interferometry," Applied Optics, 24, 3053-3058 (1985).
[35] S. K. Debnath, and M. P. Kothiyal, "Experimental study of the phase-shift miscalibration error in phase-shifting interferometry: use of a spectrally resolved white-light interferometer," Applied Optics, 46, 5103-5109 (2007).
[36] P. Hariharan, B. F. Oreb, and T. Eiju, "Digital phase-shifting interferometry: a simple error-compensating phase calculation algorithm," Applied Optics, 26, 2504-2505 (1987).
[37] J. Schmit, and K. Creath, "Extended averaging technique for derivation of error-compensating algorithms in phase-shifting interferometry," Applied Optics, 34, 3610-3619 (1995).
[38] J. Schmit, and K. Creath, "Window function influence on phase error in phase-shifting algorithms," Applied Optics, 35, 5642-5649 (1996).
[39] P. Hariharan, "Two-wavelength interferometric profilometry with a phase-step error-compensating algorithm," Optical Engineering, 45(11), 115602 (2006).